Physiol Genomics 23: 269–274, 2005.
First published September 6, 2005; doi:10.1152/physiolgenomics.00036.2005.

Comparative genomic sequence analysis coupled to chromatin immunoprecipitation: a screening procedure applied to search for regulatory elements at the *RET* locus

Francesca Puppo,[1,2] Marco Musso,[1] Doroti Pirulli,[3] Paola Griseri,[1] Tiziana Bachetti,[1,2] Sergio Crovella,[3] Giovanna Patrone,[1] Isabella Ceccherini,[1] and Roberto Ravazzolo[1,2]

[1]*Laboratory of Molecular Genetics, Giannina Gaslini Institute, Genova;* [2]*Department of Pediatrics and Center of Excellence for Biomedical Research, University of Genova; and* [3]*Department of Genetics, Institute Burlo Garofolo, Trieste, Italy*

Submitted 8 February 2005; accepted in final form 31 August 2005

Puppo, Francesca, Marco Musso, Doroti Pirulli, Paola Griseri, Tiziana Bachetti, Sergio Crovella, Giovanna Patrone, Isabella Ceccherini, and Roberto Ravazzolo. Comparative genomic sequence analysis coupled to chromatin immunoprecipitation: a screening procedure applied to search for regulatory elements at the *RET* locus. *Physiol Genomics* 23: 269–274, 2005. First published September 6, 2005; doi:10.1152/physiolgenomics.00036.2005.—*RET* gene expression is characterized by high tissue and stage specificity during the development of neural crest derivatives and in the pathogenesis of inherited cancer syndromes and Hirschsprung disease. Identifying all elements contributing to its transcriptional regulation might provide new clues to clarify both developmental and pathogenic mechanisms. We previously demonstrated that chromatin acetylation affects *RET* transcription; therefore, we have set up a strategy based on analysis of sequences conserved among species at the *RET* locus, combined with the characterization of their chromatin structure, to identify new potential regulatory elements. The histone acetylation level was evaluated by the chromatin immunoprecipitation method applied to cells displaying different degrees of endogenous *RET* expression. Real-time quantitative PCR of immunoprecipitated DNA-protein complexes and transfection experiments, with constructs expressing a reporter gene in which the putative regulatory regions are inserted, indicate a correlation between histone acetylation and endogenous *RET* expression and highlight conserved sequences with potential regulatory roles. This paper presents a reliable screening procedure to unearth elements able to affect gene regulation at the transcriptional level in a large genomic region.

Hirschsprung disease; comparative sequence analysis; histone acetylation; real-time quantitative PCR; transcriptional regulation

THE *RET* GENE ENCODES a transmembrane receptor tyrosine kinase, expressed with high tissue and stage specificity during embryo development (2). It plays a crucial role in the neural crest cells migration and differentiation to enteric sympathetic ganglia, central and peripheral nervous systems (20), and kidney development (13, 16, 25).

In humans, *RET* germline mutations are associated with different neurocristopathies: inherited cancer syndromes and Hirschsprung disease (HSCR) (12, 5). Multiple endocrine neoplasia type 2A and 2B and familial medullary thyroid carcinoma are due to constitutive activation of the *RET* protein, while HSCR phenotype is caused by haploinsufficiency or loss of function of the *RET* gene (5). In this latter case, coding sequence mutations are identified only in a limited percentage of affected individuals, suggesting that mutations in noncoding regulatory sequences might contribute to the disease phenotype by modifying the *RET* expression. Thus extending the knowledge of all elements involved in *RET* transcriptional regulation will provide new clues to clarify both developmental mechanisms and pathogenesis of the related diseases.

We have previously investigated how the regulated pattern of *RET* transcription is achieved at the molecular level by different approaches (19, 21–23). In particular, we found that histone acetylation level in two known *RET* regulatory elements, located close to the transcription start site, shows a cell line-specific pattern and correlates with endogenous gene expression (23). These results support the idea that chromatin conformation exerts a relevant control on *RET* transcription and let us establish a model for studying regulation of expression in the living cell chromatin context.

Furthermore, because it is well recognized that functional regulatory sequences tend to be more conserved across evolution than nonfunctional ones (7, 10, 26), comparative sequence analysis between orthologous sequences in different species represents a powerful tool to find important elements in noncoding genomic DNA (7, 18). *RET* expression studies in rodents (11, 25), *Drosophila* (9), and zebrafish (17) have demonstrated that the gene is expressed within comparable developmental patterns in humans and the above organisms, which further strengthens the hypothesis of conserved regulatory sequences. Very recent papers have described orthologous sequences at the human *RET* locus searching for candidate HSCR-associated variants (4, 6).

In the present work, we describe an integrated approach of sequence comparison combined with a functional assay that can be used as a general screening procedure to identify elements relevant to gene regulation. The analysis of evolutionary conservation within and surrounding the *RET* locus has been coupled to characterization of histone acetylation level and its correlation with *RET* expression in different cell types.

MATERIALS AND METHODS

Sequence analysis and comparisons. Genomic sequence comparisons with public databases were performed with Blast 2 Sequences (**http://www.ncbi.nlm.nih.gov/blast/bl2seq/wblast2.cgi**), using the following parameters: basic local alignment search tool (BLAST)N v2.2.3 (M = 1, N = −2, S = 50, Expect = 10). For this analysis, repetitive sequences were first masked (marked as unalienable) with the program Repeat Masker Web Server (**http://www.repeatmasker.org**), characterized by a large collection of different

Article published online before print. See web site for date of publication (http://physiolgenomics.physiology.org).

Address for reprint requests and other correspondence: R. Ravazzolo, Laboratory of Molecular Genetics, G. Gaslini Institute, Largo G. Gaslini, 5, 16147 Genova, Italy (e-mail: rravazzo@unige.it).

repeats from primates, rodents, other mammals, vertebrates, and *Drosophila* (A. F. A. Smit and P. Green, unpublished observations).

Global alignments of the human, mouse, and rat genomic regions were performed with the program Vista Genome Browser (**http://pipeline.lbl.gov/index.html**), using a window size of 100 bp and a conservation level of 75%.

Cell cultures and transfections. IMR32 (human neuroblastoma cells) were grown in RPMI medium (Roswell Park Memorial Institute, Hyclone); MTC-TT, human medullary thyroid carcinoma, in Ham's F-12 medium (nutrient mixture for Hamster F-12, Hyclone); and Neuro2A, murine neuroblastoma, in DMEM (Sigma). All media were supplemented with 10% fetal bovine serum (FBS; GIBCO), 2 mM L-glutamine, 100 U/ml penicillin, and 100 μg/ml streptomycin at 37°C in a humidified atmosphere with 5% CO_2.

Neuro2A (1.2×10^5 cells) and MTC-TT (2×10^5 cells) were plated in 35-mm-diameter dishes and transfected 24 h after plating using PEI (Sigma) or Lipofectamine 2000 (Invitrogen), respectively, with 400 ng of pGL3 promoter or pRET vectors or an equimolar ratio of pSV40-H, pSV40-I, pRET-H, and pRET-I. Plasmid pBluescript KS(-) (Stratagene) was used to keep up to 1 μg the total DNA amount, and 100 ng of renilla luciferase reporter plasmid (pRL-SV40, Promega) were added to each sample as an internal control for transfection efficiency. Luciferase and renilla activity was assayed with the Dual-Luciferase Reporter Assay System (Promega) on a TD 20/20 luminometer (Turner Designs). Three independent transfection experiments were performed in triplicate.

Chromatin immunoprecipitation assay. Cell nuclei from IMR32 and MTC-TT were isolated and micrococcal nuclease digested as previously described (23). Chromatin fragments were preincubated with 50 μl of protein A-sepharose (Amersham Pharmacia Biotech) to reduce background caused by nonspecific adsorption of DNA-protein complexes to protein A-sepharose beads. Immunoprecipitation was then performed with antibodies against tetra-acetylated histone H4, as we already reported (23). DNA isolated from antibody bound and unbound fractions was extracted twice with phenol-chloroform. Three independent chromatin immunoprecipitation (ChIP) assays were performed for each cell line.

Real-time PCR quantification analysis of immunoprecipitated DNA. Real-time PCR quantification of immunoprecipitated DNA was carried out with the SYBR Green PCR Master Mix (Applied Biosystems) and primers designed to obtain PCR products with length ranging between 150 and 200 bp (Table 1). Immunoprecipitated fractions were estimated by human β-actin housekeeping gene amplification with the primers described in the Table 1, using ABI Prism 7700 Sequence Detection System (Applied Biosystems), and each product was compared with a standard curve of human genomic DNA (Taq Man DNA Template Reagents, Applied Biosystems).

The relative proportions of immunoprecipitated fragments were determined using the ΔCt comparative method based on the threshold cycle (Ct) value for each PCR reaction (8) (ABI Prism 7700 Sequence Detection System User Bulletin, Applied Biosystems). The ΔCt of each amplimer was obtained by subtracting the Ct value of *RET* exon 12 PCR product (endogenous reference), assuming a nonsignificant influence of histone acetylation at this level. A ΔΔCt value was then calculated by subtracting the ΔCt for the bound fraction to ΔCt of the unbound fraction (calibrator). Real-time PCR amplification was performed in triplicate and repeated at least three times.

A list of all the fragments amplified by quantitative PCR and their specific primer pairs are included in Table 1. Cycling parameters are as follows: 15 s at 95°C, 60 s at 60°C, and 30 s at 72°C for all the conserved noncoding sequences (CNS; *A–I*) and exon 12 amplimers; 30 s at 95°C, 30 s at 63°C, and 30 s at 72°C to amplify enhancer site SOX10/PAX3 (SPX) and β-actin; and 30 s at 95°C, 30 s at 68°C, 30 s at 72°C, and 10% glycerol to obtain the minimal promoter amplification. All the PCR reactions were at least 40 cycles long.

Table 1. *CNS and qPCR analysis*

Fragment	Human/Mouse Conservation, %	Human/Rat Conservation, %	Size, bp	*Position, bp	qPCR Primers	Primer Sequence 5′ → 3′
A	81	80	153	−20,630	*A*for	CCCTGCAGTGAACTCAGATCC
					*A*rev	CAGGCTGTTTCTGGGAAGCA
B	76		108	−15,080	*B*for	ACCGCCAAGCCATTACTCAC
					*B*rev	AATCCTTGGAATCTCCTTCGG
C		83	126	−11,220	*C*for	TCTCTTCTTCATTGACTGGGAGACATTT
					*C*rev	GCTGGCCTGCGCATTATT
D	79	78	184	−8,690	*D*for	TCTCCTCTCTCTGGCTCAGGG
					*D*rev	CTGCTGAGGCTTCCAGAGGT
E	80	81	111	−8,135	*E*for	TGAGGTCTTCCAAACCTTCCA
					*E*rev	GCTTCCTTTTCCAGGTTCCC
F	85	87	325	−5,110	*F*for	GGCTGTATAGGAAGTGTGTATTGAACA
					*F*rev	AAAATAGGCCTTAATGGATCTTTGC
G	86	87	137	−1,110	*G*for	CAAGCCAGCCTCTGTCTTGG
					*G*rev	TTGCTGTGTGCAGAACCCC
H	79	80	223	+2,890	*H*for	TGCAAGCAGAGAGCAAATGG
					*H*rev	TCCTCCACTGGCTAAAGGCT
I	88	90	163	+9,460	*I*for	CACTTGGGTGGCCAGTCCT
					*I*rev	GCTCCTGCCCAACTGCAAT
SPX Enh	under 50	under 50	700	−3,390	SPX1for	TGTGGGGACATGGAAAACTG
					SPX1rev	GCATTCCTGGAACTGCTG
MinProm	63	60	140	−140	qPMfor	CGCAGCCAGAGCAAGCAC
					qPMrev	GCTTCGGTCGCGGGACT
Exon 12	90	88	148	+30,650	qE12for	TCTTCTCCCCCTTCCCTCAT
					qE12rev	CCCTGCTCTGCCTTTCAGAT
β-Actin					bact1F	TCACCCACACTGTGCCCATCTACGA
					bact1C	CAGCGGAACCGCTCATTGCCAATGG

Conserved noncoding sequences (CNS) and quantitative PCR (qPCR) analysis. For each of the selected CNS, the % conservation between human and mouse and human and rat and the relative size and position from the human transcriptional start site (*) are reported. A list of all fragments amplified by qPCR and their specific primer pairs are included. Cycling parameters are reported in MATERIALS AND METHODS. MinProm, minimal promoter; SPX Enh, enhancer site SOX10/PAX3; for, forward; rev, reverse.

Plasmid construction. Genomic fragments corresponding to the *H* and *I* regions were cloned downstream from the luciferase reporter gene, either driven by SV40 promoter (pGL3 promoter, Promega) or *RET* minimal promoter (−143, +53) as previously described (22). In particular, the *H* region corresponding to the intron 1 sequence spanning from nucleotide +2,892 to +3,896, was amplified from genomic DNA by PCR using primers *H* forward (*H*F; 5′-CGCGGATCCACGCGTCTGGCCTCCAGAAGCTGCC-3′) and *H* reverse (*H*R; 5′-CCAATCCGTCGACCCTTGTCTTCAGAGCAG) and then cut and cloned into *BamH*I site (pSV40-H and pRET-H). The *I* region, ranging from nucleotide +9,064 to +9,756, was amplified using primers *I*F (5′-CCAGGGTCGACTGCAGCTTAATTCCTAGCC-3′) and *I*R (5′-CATACGTCGACCCAGACCAGCTGCAGCGGC -3′) and then cut and cloned into *Sal*I site (pSV40-I and pRET-I). Finally, all constructs were controlled by sequencing of the entire length of the cloned DNA fragment.

Statistical analysis. In ChIP and transfection experiments, statistical significance of results was determined by Student's *t*-test, available online (Tools for Science, Statistics; **http://www.physics.csbsju.edu/stats**).

RESULTS

Sequence conservation in the RET locus. We initially performed a comparative sequence analysis in the attempt to identify conserved noncoding elements located inside the *RET* gene locus that could potentially play a role in gene expression regulation. We submitted the human (NT_033985), mouse (NT_039353), rat (NW_047696), *Drosophila* (NG_000430), and pufferfish (*Tetraodon fluviatilis,* TFU58673) *RET* orthologous gene sequences to the Repeat Masker Web Server (**http://www.repeatmasker.org/**) and performed alignments between the masked regions by Blast 2 Sequence (**http://www.ncbi.nlm.nih.gov/blast/bl2seq/bl2.html**). The human sequence started from 100 kb upstream of the transcription start site and, for the other orthologous genes, from the largest available upstream sequence. Most of the resulting exons were conserved, in particular those encoding the tyrosine kinase domain, in all analyzed species, whereas we did not observe high conservation between human and *Drosophila* or zebrafish in noncoding regions (data not shown).

The following comparison was carried out with the Vista Genome Browser (**http://pipeline.lbl.gov/index.html**) software and limited to human, mouse, and rat orthologs. Figure 1 reports the results on a region starting from −20 kb with respect to the transcription start site, up to the conserved part of intron 1 of human *RET* (+10.6 kb): peaks in murine and rat regions, having >50% conservation with respect to human sequence, are represented. Regions displaying at least 75% identity and over 100 bp in length are differently colored: pink peaks are CNS, while blue peaks are exons. Several regions upstream of the gene and two regions within the first intron are highly conserved and remarkably similar between human,

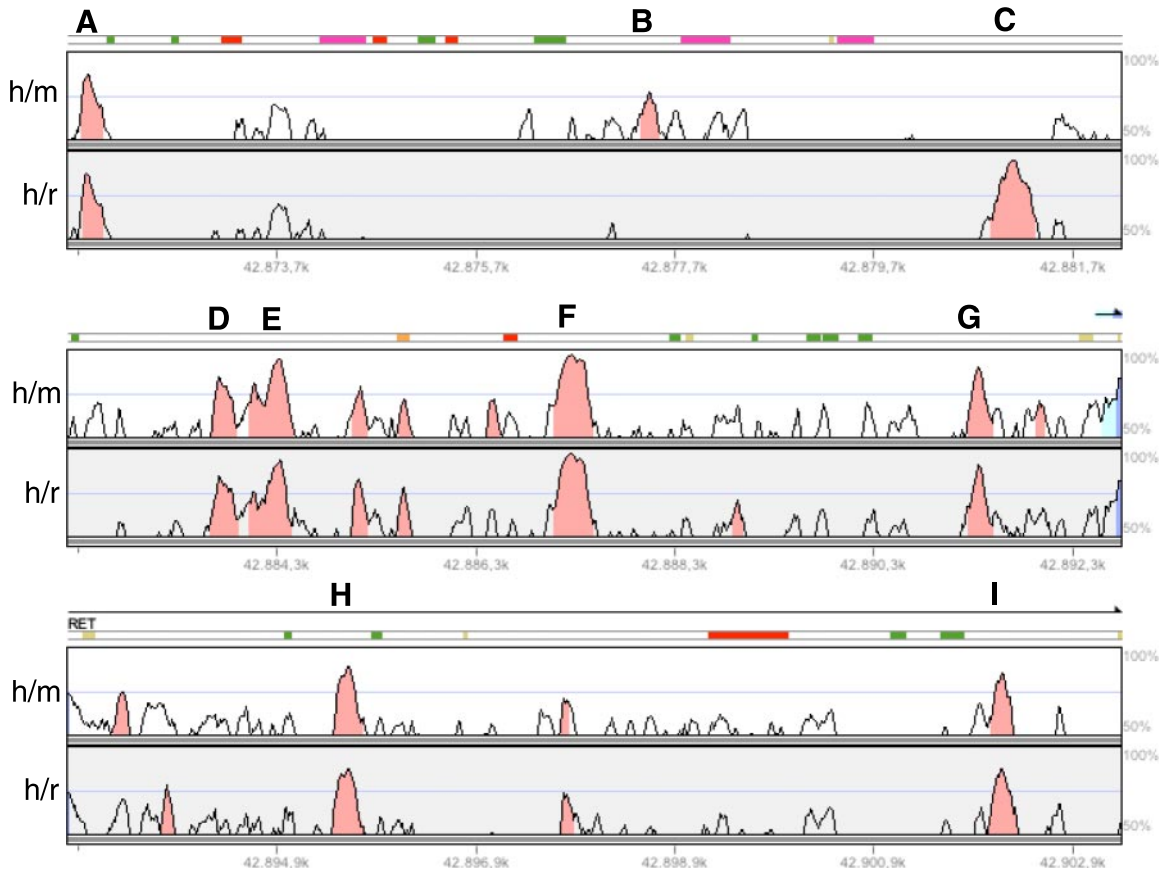

Fig. 1. Map of the sequence conservation in the *RET* genomic region. Results of analysis performed by the web-based alignment program Vista Genome Browser (**http://pipeline.lbl.gov/index.html**) in a genomic region encompassing DNA sequence from −20 to +10.6 kb. The peak corresponding to the first exon is marked in blue. Conserved noncoding sequences (CNS) >100 bp with >75% identity are marked in pink. Selected CNS are indicated with capital letters (from *A* to *I*). The *top* box in each row refers to human/mouse comparison (h/m) and the *bottom* to human/rat (h/r).

mouse, and rat. This allowed us to select nine fragments, indicated from *A* to *I* in Fig. 1 and Table 1.

Comparison of histone acetylation profiles among cell lines with differential RET expression. To test whether conserved sequences *A–I* might play a regulatory role in gene transcriptional regulation, we have performed ChIP on two different cell lines. These were chosen on the basis of their endogenous *RET* mRNA expression and transcription: the neuroblastoma IMR32 cell line, expressing *RET* at low levels, and the medullary thyroid carcinoma MTC-TT cell line, displaying a high level of *RET* transcription (22, 23). We have quantified the histone acetylation level in the selected regions by collecting DNA fragments bound to tetra-acetylated histone H4 (antibody-bound fraction) and performing Taq Man real-time PCR with specific pairs of primers (Table 1). The values obtained for each genomic region under analysis were compared with those of a *RET* exon 12 amplimer taken as an endogenous reference and assumed to be unaffected by differential acetylation levels in the two *RET*-expressing cell lines. Bound fraction values were compared with those of the unbound fraction for each fragment amplified. Figure 2 shows the strong correlation between histone acetylation and endogenous *RET* expression in each cell line: IMR32 cells showed a globally low histone acetylation, with the exception of the *RET* minimal promoter; MTC-TT cells showed higher acetylation levels compared with IMR32, with significant difference in several of the amplified fragments. In particular, as depicted in Fig. 2, the SOX10/PAX3 enhancer (22, 23) and the *G*, *H*, and *I* regions showed more than twofold higher acetylation, with a striking difference at the *H* region.

Assay of regulatory activity. Functional assays on the region upstream of the *RET* transcription start point have been reported by a number of authors (1, 14, 22) who did not indicate particular regions of interest except for a target sequence for the Sox10 and Pax3 transcription factors and a proximal promoter sequence. Moreover, no molecular variants are located in the *A*-to-*G* upstream conserved sequences. Therefore, we have extended the functional characterization of the two intronic sequences, indicated as *H* and *I*, which showed different acetylation levels between the two tested cell lines, by performing transient transfection experiments with reporter plasmids. Two sets of constructs have been prepared: *1*) luciferase expression plasmids driven by the *RET* minimal promoter, containing either the *H* or the *I* sequences placed downstream of the luciferase coding sequence, and *2*) luciferase expression plasmids driven by the SV40 promoter, containing either the *H* or the *I* sequences placed downstream of the reporter gene. Both sets of constructs were transfected in Neuro2A murine neuroblastoma and MTC-TT cell lines. Figure 3 reports results showing that the two regions were able to enhance promoter activity when coupled to the SV40 promoter in both cell lines, with higher enhancer activity for the *I* region. When the two regions were coupled to the *RET* minimal promoter, enhancer activity was confirmed for the *I* region.

DISCUSSION

The study of the *RET* gene transcriptional regulation, although already approached by different methodologies (1, 14, 15, 19, 21–23), has not yet provided exhaustive information about *cis*- and *trans*-acting factors involved in specific control of gene expression during the critical stages of embryo development and in the appropriate cell types. Identification of sequences and factors crucial in such a functional process is fundamental not only to understand the physiological steps that lead to the definition of some organs and tissues but also to explain results of genetic studies that point to a region at the 5′-end of the *RET* gene as the location of a functional variant predisposing to Hirschsprung disease (3, 4, 6, 24). Following the hypothesis that this variant affects the *RET* gene transcription and, by consequence, the level of its expression, the present work was undertaken with the objective to discover *cis*-elements possibly participating in the regulatory mechanisms. The strategy for our investigation was based on the knowledge that enhancers and other noncoding sequences important for gene expression control tend to be conserved

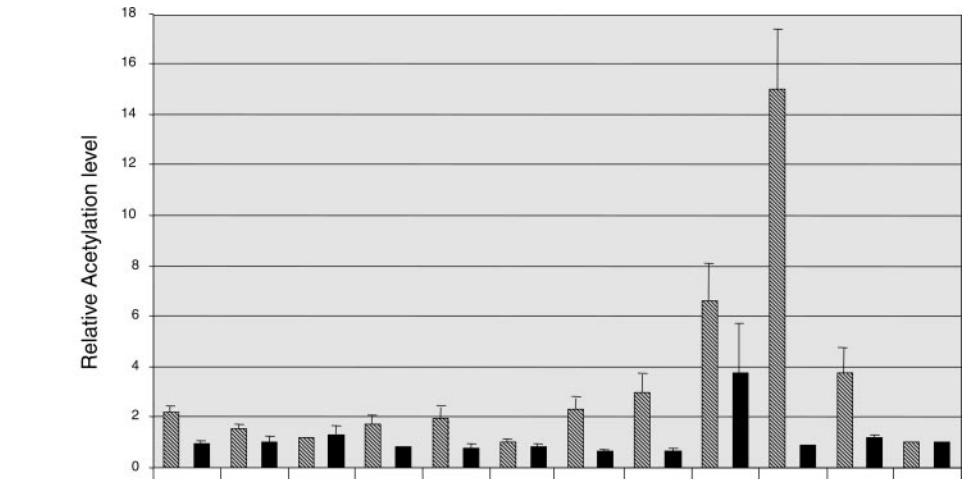

	A	B	C	D	E	F	Sox10/ Pax3	G	Min Prom	H	I	Exon12
MTC-TT	2,188	1,568	1,164	1,734	1,977	1,032	2,307	3,001	6,581	15,02	3,757	1
IMR32	0,935	1,035	1,330	0,825	0,785	0,845	0,648	0,675	3,740	0,903	1,203	1

Fig. 2. Quantification of histone acetylation after chromatin immunoprecipitation (ChIP) from IMR32 and MTC-TT cells. Bars indicate the relative histone H4 acetylation level at the conserved sequences (*A–I*), the enhancer site SOX10/PAX3 (SPX Enh), the minimal promoter (Min Prom), and exon 12, analyzed by real-time PCR. Solid bars represent values obtained from IMR32 cells, whereas hatched bars are those from MTC-TT cells. Means ± SE are given for at least 3 separate experiments.

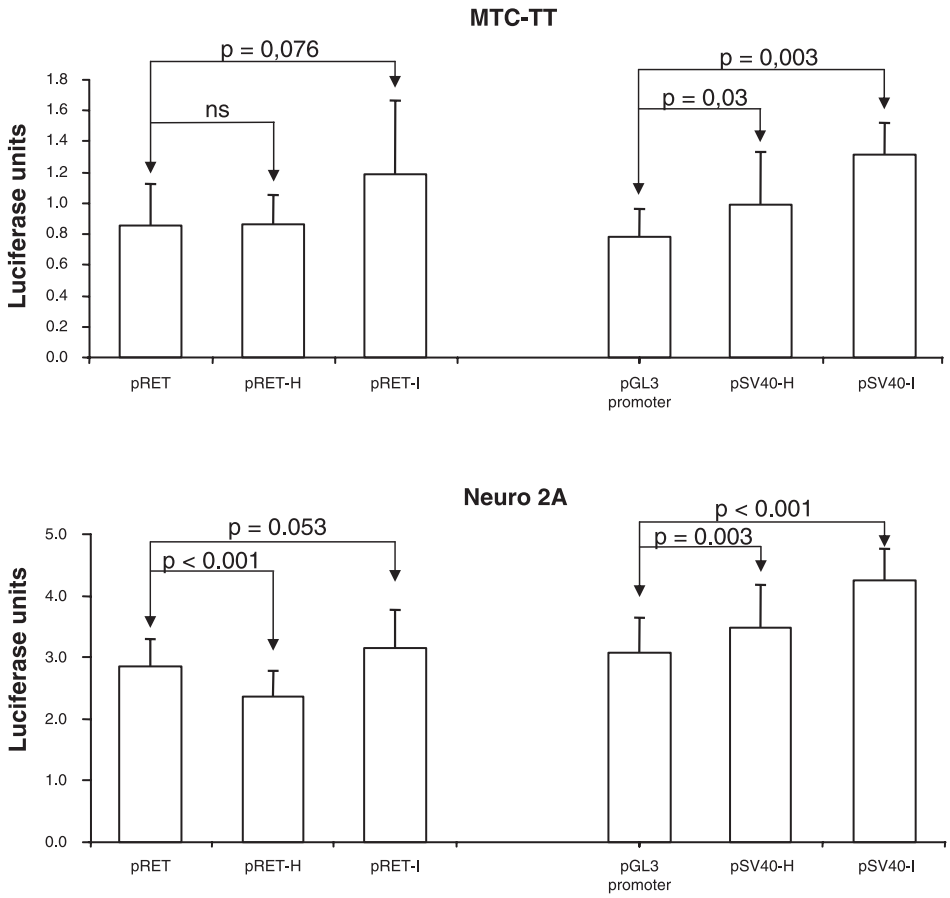

Fig. 3. Regulatory activity of *H* and *I* regions Results of transfection experiments in MTC-TT and Neuro2A cell line with the indicated reporter expression constructs. The *y*-axes report luciferase units at different scales for the 2 different cell types. Each bar indicates mean (SD) of 3 experiments performed in triplicate. Statistical significance is reported as *P* value.

across evolution. Consequently, we carried out a comparative analysis of genomic orthologous sequences from evolutionarily diverged species, in a wide *RET* genomic region. Cross-species comparison resulted in the identification of seven conserved noncoding regions upstream of the transcription start site and two regions within the first intron. We are aware that comparative analysis might provide further information according to progress and accuracy in the rat and mouse sequences available in databases as well as in other yet poorly investigated species. With the aim to validate a screening method able to unearth regulatory elements, we have applied a functional assay to verify the starting hypothesis, for those sequences satisfying the selection criteria. This has been carried out by ChIP analysis with an accurate quantitative evaluation of histone acetylation performed by real-time PCR.

We chose to compare MTC-TT cells, which express a high level of *RET* mRNA, with IMR32 cells, which display a low level of *RET* mRNA: consistently, MTC-TT globally showed a higher level of histone acetylation in most of the conserved fragments.

The most significant difference between the two cell lines in the 5′-flanking region was observed at the already described SOX10/PAX3 enhancer (14, 15) as well as at the *G* sequence, which was never reported either as an established or as a putative regulatory sequence. The *RET* minimal promoter did not show a striking difference between the two cell lines, and its association with hyperacetylated H4 histones resulted in elevated levels in both cell types, as might be expected in a promoter region that is essential also for basal level of gene.

The *H* and *I* sequences, both located in intron 1, showed the most significant differences between MTC-TT and IMR32. Results obtained by transient transfection experiments with constructs expressing the luciferase reporter gene under control of two different promoters and the above putative regulatory elements raise a number of observations. The *H* and *I* regions show regulatory activity, as shown by statistical significance of data, thus confirming the results obtained by the ChIP analysis. These results vary according to the type of construct, which is not surprising when considering the huge variability of results present in the scientific literature on reporter assays performed with even slightly different constructs or the same constructs in different cell lines. While this article was under revision, results on the role of the *I* sequence have been described showing that this region could enhance SV40 promoter activity by ~30-fold, in the conditions used in those experiments (6). Our results differ in the level of enhancing activity displayed by the *I* region, which may be due to different types of constructs utilized in transfection experiments and the position of the putative enhancer element inside the plasmid: downstream of the luciferase coding sequence instead of upstream of the promoter sequence. Moreover, considering the entire examined region, we cannot exclude that the use of different antibodies in ChIP analysis, of other cell lines reflecting epigenetic regulation specific to different tissues and differentiation stages, and of other constructs and cell lines in transfection experiments could reveal some other elements able to contribute to the gene transcriptional control. In this regard, it is very difficult and questionable to evaluate how a single

element contributes to regulation of transcription, considering that it could be the result of a combined effect of different elements, in the endogenous chromatin context of an extended genomic region.

These observations should warn against taking single assays as unique proof of a functional role and suggest adoption of integrated strategies in which different experimental approaches are used to support initial hypotheses such those raised by genetic evidences. This applies well to the field of HSCR susceptibility, in which several genetic evidences (3, 4, 6) suggest that one or more responsible functional variant(s) is located in the genomic region that we and others have investigated.

We believe that the described experimental approach, based on the combined analysis of sequence conservation and chromatin conformation assessed by ChIP and quantitative real-time PCR, applied to a large *RET* genomic region, has proved to be very useful as a screening procedure to highlight and characterize potential regulatory elements, defining their tissue specificity and chromatin conformation dependence. Such an approach has led us to identify candidate regions in which the search for molecular variants with functional significance is worth addressing, contributing to a further understanding of the molecular basis of *RET* expression regulation and disease susceptibility. Furthermore, this strategy can be generally used to unearth transcriptional enhancers/silencers in wide genomic regions, provided suitable cell types can be used as a source of chromatin.

ACKNOWLEDGMENTS

The administrative assistance of Loredana Velo is greatly acknowledged.

GRANTS

This work was supported by TELETHON Grant GGP04257 to I. Ceccherini, European Community Contract No. QLG1-2001-01646 to I. Ceccherini, a Banco San Paolo contribution to I. Ceccherini, and an Italian Ministry of University and Research-Investment Fund for Basic Research (FIRB) Grant to R. Ravazzolo.

REFERENCES

1. **Andrew SD, Delhanty PJ, Mulligan LM, and Robinson BG.** Sp1 and Sp3 transactivate the RET proto-oncogene promoter. *Gene* 256: 283–291, 2000.
2. **Attie-Bitach T, Abitbol M, Gerard M, Delezoide AL, Auge J, Pelet A, Amiel J, Pachnis V, Munnich A, Lyonnet S, and Vekemans M.** Expression of the RET proto-oncogene in human embryos. *Am J Med Genet* 80: 481–486, 1998.
3. **Burzynski GM, Nolte IM, Osinga J, Ceccherini I, Twigt B, Maas S, Brooks A, Verheij J, Menacho IP, Buys CH, and Hofstra RM.** Localizing a putative mutation as the major contributor to the development of sporadic Hirschsprung disease to the RET genomic sequence between the promoter region and exon 2. *Eur J Hum Genet* 12: 604–612, 2004.
4. **Burzynski GM, Nolte IM, Bronda A, Bos KK, Osinga J, Plaza Menacho I, Twigt B, Maas S, Brooks AS, Verheij JB, Buys CH, and Hofstra RM.** Identifying candidate Hirschsprung disease-associated RET variants. *Am J Hum Genet* 76: 850–858, 2005.
5. **Chakravarti A and Lyonnet S.** Hirschsprung disease. In: *The Metabolic and Molecular Bases of Inherited Disease*, edited by Scriver C, Beaudet AL, Sly WS, and Valle D. New York: McGraw-Hill, 2001, p. 6231–6255.
6. **Emison ES, McCallion AS, Kashuk CS, Bush RT, Grice E, Lin S, Portnoy ME, Cutler DJ, Green ED, and Chakravarti A.** A common sex-dependent mutation in a RET enhancer underlies Hirschsprung disease risk. *Nature* 434: 857–863, 2005.
7. **Ge B, Li O, Wilder P, Rizzino A, and McKeithan TW.** NF-κB regulates BCL3 transcription in T lymphocytes through an intronic enhancer. *J Immunol* 171: 4210–4218, 2003.
8. **Griseri P, Bachetti T, Puppo F, Lantieri F, Ravazzolo R, Devoto M, and Ceccherini I.** A common haplotype at the 5′ end of the RET proto-oncogene, over-represented in Hirschsprung patients, is associated with reduced gene expression. *Hum Mutat* 25: 189–195, 2005.
9. **Hahn M and Bishop J.** Expression pattern of Drosophila ret suggests a common ancestral origin between the metamorphosis precursors in insect endoderm and the vertebrate enteric neurons. *Proc Natl Acad Sci USA* 98: 1053–1058, 2001.
10. **Hardison RC, Oeltjen J, and Miller W.** Long human-mouse sequence alignments reveal novel regulatory elements: a reason to sequence the mouse genome. *Genome Res* 7: 959–966, 1997.
11. **Honda T, Yokota S, Gang FG, Takahashi M, and Sugiura Y.** Evidence for the c-ret protooncogene product (c-Ret) expression in the spinal tanycytes of adult rat. *J Chem Neuroanat* 17: 163–168, 1999.
12. **Ichihara M, Murakumo Y, and Takahashi M.** RET and neuroendocrine tumors. *Cancer Lett* 204: 197–211, 2004.
13. **Kawakami T, Wakabayashi Y, Aimi Y, Isone T, and Okada Y.** Developmental expression of glia cell-line derived neurotrophic factor, neurturin, and their receptor mRNA in the rat urinary bladder. *Neurourol Urodyn* 22: 83–88, 2003.
14. **Lang D, Chen F, Milewski F, Li J, Lu MM, and Epstein J.** Pax3 is required for enteric ganglia formation and functions with Sox10 to modulate expression of c-Ret. *J Clin Invest* 106: 963–971, 2000.
15. **Lang D and Epstein J.** Sox10 and Pax3 physically interact to mediate activation of a conserved c-RET enhancer. *Hum Mol Genet* 12: 937–945, 2003.
16. **Majumdar A, Vainio S, Kispert A, McMahon J, and McMahon AP.** Wnt11 and Ret/Gdnf pathways cooperate in regulating ureteric branching during metanephric kidney development. *Development* 130: 3175–3185, 2003.
17. **Marcos-Gutierrez CV, Wilson SW, Holder N, and Pachnis V.** The zebrafish homologue of the ret receptor and its pattern of expression during embryogenesis. *Oncogene* 14: 879–889, 1997.
18. **Miller W.** So many genomes, so little time. *Nat Biotechnol* 18: 148–149, 2000.
19. **Munnes M, Patrone G, Schmitz B, Romeo G, and Doerfler W.** A 5′-CG-3′-rich region in the promoter of the transcriptionally frequently silenced RET protooncogene lacks methylated cytidine residues. *Oncogene* 17: 2573–2583, 1998.
20. **Natarajan D, Marcos-Gutierrez C, Pachnis V, and deGraaff E.** Requirement of signalling by receptor tyrosine kinase RET for the directed migration of enteric nervous system progenitor cells during mammalian embryogenesis. *Development* 129: 5151–5160, 2002.
21. **Patrone G, Puliti A, Bocciardi R, Ravazzolo R, and Romeo G.** Sequence and characterisation of the RET proto-oncogene 5′ flanking region: analysis of retinoic acid responsiveness at the transcriptional level. *FEBS Lett* 419: 76–82, 1997.
22. **Patrone G, Puppo F, Scaranari M, Cusano R, Griseri P, Romeo G, Ceccherini I, Puliti A, and Ravazzolo R.** Cell-line specific transcription rates of the RET gene and functional domains in its minimal promoter. *Gene Funct Dis* 3: 145–153, 2000.
23. **Puppo F, Griseri P, Fanelli M, Schena F, Romeo G, Pelicci PG, Ceccherini I, Ravazzolo R, and Patrone G.** Cell-line specific chromatin acetylation at the Sox10-Pax3 enhancer site modulates the RET proto-oncogene expression. *FEBS Lett* 523: 123–127, 2002.
24. **Sancandi M, Griseri P, Pesce B, Patrone G, Puppo F, Lerone M, Martucciello G, Romeo G, Ravazzolo R, Devoto M, and Ceccherini I.** Single nucleotide polymorphic alleles in the 5′ region of the RET proto-oncogene define a risk haplotype in Hirschsprung's disease. *J Med Genet* 40: 714–718, 2003.
25. **Schuchardt A, D'Agati V, Pachnis V, and Costantini F.** Renal agenesis and hypodysplasia in ret-k-mutant mice result from defects in ureteric bud development. *Development* 122: 1919–1929, 1996.
26. **Touchman JW, Dehejia A, Chiba-Falek O, Cabin DE, Schwartz JR, Orrison BM, Polymeropoulos MH, and Nussbaum RL.** Human and mouse α-synuclein genes: comparative genomic sequence analysis and identification of a novel gene regulatory element. *Genome Res* 11: 78–86, 2001.